Meson production in high-energy electron-nucleus scattering

Göran Fäldt*
Department of Physics and Astronomy, Uppsala University, Box 516, S-751 20 Uppsala, Sweden
(Received 24 February 2012; revised manuscript received 2 July 2012; published 28 August 2012)

Pseudoscalar mesons can be produced and studied in high-energy electron-nucleus scattering. We review and extend our previous theoretical analysis of meson production in the nuclear Coulomb field. The $P \to \gamma\gamma$ decay rates are most directly determined for mesons produced in the double-Coulomb region where both photons are nearly real, and provided the hadronic-background contributions remain small. The larger the mass of the meson the higher the electron energy needed to assure such favorable conditions.

DOI: 10.1103/PhysRevC.86.024611 PACS number(s): 24.10.Ht, 25.20.Lj, 25.30.Rw, 13.60.Le

I. INTRODUCTION

Pseudoscalar mesons are produced in high-energy electron-nucleus scattering through a two-photon-fusion process where the two photons are radiated, one by the high-energy electron and the other by the atomic nucleus. This possibility was studied, in the Born approximation, by Hadjimichael and Fallieros [1]. Recently, a Glauber-model [2] description of the same process has been developed [3]. Theoretical studies of the two-photon-fusion process are particularly valuable since the PrimEx Collaboration [4] aims at measuring electromagnetic properties of pseudoscalar mesons through this effect, in 11 GeV/c electron-nucleus scattering.

The kinematics of the electron-nucleus-meson-production reaction is defined through

$$e^-(k_1) + \mathrm{A}(p_1) \to e^-(k_2) + P(K) + A(p_2), \qquad (1)$$

where P represents one of the mesons π^0, η, or η'. Our analysis is relevant for high electron and meson energies and small transverse momenta. In addition, the momentum transfers to meson and nucleus should preferentially be in the double-Coulomb region, leading to further kinematic restrictions. The mechanism dominating this region is, at sufficiently high energies, described by the graph of Fig. 1. This graph shows that pion-nucleus photoproduction is a subgraph of the pion-nucleus electroproduction, but only in special kinematic circumstances does the photoproduction amplitude enter as a separate factor. Our treatment of the electroproduction amplitude is similar to our previous treatment of the photoproduction amplitude [5].

The cross-section distribution is in the Coulomb region mainly determined by the photon propagators, which lead to structures like

$$\frac{k_\perp}{\mathbf{k}_\perp^2 + k_\parallel^2/\gamma^2}, \qquad (2)$$

with $\mathbf{k}_\perp$ the variable photon transverse momentum, $k_\parallel$ the fixed photon longitudinal momentum, and γ the gamma factor of the radiating charge. This behavior results in a cross-section maximum at $k_\perp = k_\parallel/\gamma$, the Primakoff peak. For the low-energy photon radiated by the nucleus $k_\parallel/\gamma = m_P^2/2K_\parallel$, where m_P is the mass of the meson and $K_\parallel = \mathbf{K}\cdot\hat{k}_1$ its longitudinal (or total) momentum. This expression is well known from ordinary Coulomb production. For the high-energy photon radiated by the high-energy electron the effective longitudinal momentum is $k_\parallel/\gamma = m_e$, with m_e the electron mass.

In the PrimEx experiment [4] typical energies are as follows: for the incident electron $E(\mathbf{k}_1) = 11$ GeV, for the scattered electron $E(\mathbf{k}_2) = 300$ MeV, and for the pseudoscalar meson $\omega(\mathbf{K}) = 10.7$ GeV. Consequently, the energy of the virtual photon radiated by the electron, and initiating the meson production through fusion with a soft photon radiated by the nucleus, is also 10.7 GeV. These numbers are only for numerical illustration. The model we present is in itself a general one.

The electron-coherent-nucleus-production amplitude is a sum of two amplitudes: the two-photon-fusion amplitude $\mathcal{M}_{2\gamma}$ of Fig. 1, and the electron-induced hadronic-photoproduction amplitude $\mathcal{M}_\gamma$ of Fig. 2.

Normalizations are chosen such that in the Born approximation the unpolarized cross-section distribution for the two-photon-fusion contribution simplifies to

$$\frac{d\sigma}{d^2k_{2\perp}d^2K_\perp dk_{2\parallel}} = \frac{1}{\pi K_\parallel}\left[\frac{Z\alpha^2}{m_\pi}g_{\pi\gamma\gamma}\,\frac{q_\perp}{\mathbf{q}_\perp^2 + m_e^2}\cdot\frac{Q_\perp}{\mathbf{Q}_\perp^2 + Q_\parallel^2}\right]^2, \qquad (3)$$

with $-Q_\parallel = m_P^2/2K_\parallel$. The structure of the cross-section distribution at small-transverse momenta is essentially determined by the photon-exchange propagators. There are two such propagators: one in the variable $\boldsymbol{q}_\perp$, and one in the variable $\boldsymbol{Q}_\perp$. Each of them exhibits a Primakoff-peak structure. We observe that the spin-averaged Born approximation does not depend on the angle between the transverse momenta $\mathbf{q}_\perp$ and $\mathbf{Q}_\perp$.

The numerical illustrations in Ref. [3] erroneously employ positive values for $Q_\parallel$. However, this error is of no concern since the quantities graphed are independent of the sign of $Q_\parallel$.

II. CLASSICAL RADIATION BY RELATIVISTIC ELECTRONS

The pseudoscalar-meson decay $P \to \gamma\gamma$ is governed by the Hamiltonian density

$$\mathcal{H}(x) = \tfrac{1}{2}g\,\mathbf{E}(x)\cdot\mathbf{B}(x)P(x), \qquad (4)$$

*goran.faldt@physics.uu.se

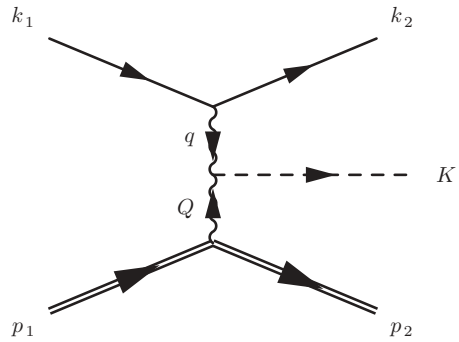

FIG. 1. Graph describing pseudoscalar-meson production in the Coulomb field of a nucleus in electron coherent-nucleus scattering.

with coupling constant $g = e^2 g_{P\gamma\gamma}/m_P$. In our application the electromagnetic fields are generated by the electron and nuclear charges. It is therefore instructive first to review the classical counterparts of these fields [6].

A point particle of charge e moves along the trajectory $\mathbf{r}(t) = \mathbf{r}_0 + \mathbf{v}t$. The plane-wave decompositions of the associated electric and magnetic fields are

$$\mathbf{E}(\mathbf{k}, t) = ie\frac{-\mathbf{k} + (\mathbf{k}\cdot\mathbf{v})\mathbf{v}}{\mathbf{k}^2 - (\mathbf{k}\cdot\mathbf{v})^2}e^{-i\mathbf{k}\cdot\mathbf{r}(t)}, \tag{5}$$

$$\mathbf{B}(\mathbf{k}, t) = ie\frac{\mathbf{k}\times\mathbf{v}}{\mathbf{k}^2 - (\mathbf{k}\cdot\mathbf{v})^2}e^{-i\mathbf{k}\cdot\mathbf{r}(t)}. \tag{6}$$

The denominators can be rewritten as

$$\mathbf{k}^2 - (\mathbf{k}\cdot\mathbf{v})^2 = \mathbf{k}_\perp^2 + k_\parallel^2/\gamma^2, \tag{7}$$

with $\gamma = E/m$ the relativistic gamma factor of the charged particle. Transverse and parallel refer to directions orthogonal and parallel to the velocity $\mathbf{v}$ of the charged particle. The numerators, on the other hand, may be rewritten as

$$\mathbf{k} - (\mathbf{k}\cdot\mathbf{v})\mathbf{v} = (\mathbf{k}_\perp, k_\parallel/\gamma^2), \tag{8}$$

$$\mathbf{k}\times\mathbf{v} = \mathbf{k}_\perp\times\mathbf{v}. \tag{9}$$

In the application to the PrimEx experiment two limits are of interest. The nonrelativistic limit, $v \ll 1$, applies to the soft radiation by the nucleus, when the denominators of Eqs. (5) and (6) reduce to $\mathbf{k}^2$. The other limit applies to hard radiation by the ultrarelativistic electron, where in the denominators the longitudinal momentum $k_\parallel$ is cut down by the Lorentz factor $1/\gamma$.

In the PrimEx experiment there are kinematic restrictions. The longitudinal momentum of the soft photon is fixed to be $m_P^2/2K_\parallel$, with $K_\parallel$ the meson momentum. The longitudinal momentum of the hard photon is very nearly equal to the momentum of the electron, so that $k_\parallel/\gamma \approx m_e$. Thus, these two parameters act as cutoffs for the corresponding transverse momentum distributions. The longitudinal component of the electric field, Eq. (5), is for the hard photon cut down by the factor $1/\gamma^2$ and may be neglected.

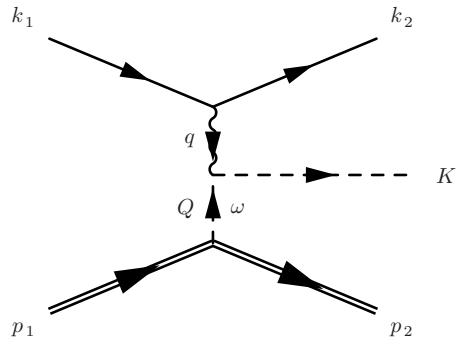

FIG. 2. Graph describing the hadronic contribution to pseudoscalar-meson production in electron coherent-nucleus scattering. Dominant contribution from ω exchange.

III. THE COULOMB CONTRIBUTION

We shall now review the formulas for the Coulomb contribution to electron-induced pion production, i.e., the two-photon-fusion amplitude of Fig. 1. The corresponding cross-section distribution has a double-peak-Primakoff structure. We normalize so that the cross-section distribution takes the form

$$\frac{d\sigma}{d^2k_{2\perp}d^2K_\perp dk_{2\parallel}} = \frac{1}{\pi K_\parallel}[u^\dagger(k_2)\mathcal{M}_{2\gamma}u(k_1)]^2, \tag{10}$$

where $u(k_1)$ and $u(k_2)$ are two-component spinors for incident and scattered electrons. The two-photon amplitude is decomposed as

$$\mathcal{M}_{2\gamma} = i\mathcal{N}_{2\gamma}\,[G(\mathbf{q},\mathbf{Q}) - H(\mathbf{q},\mathbf{Q})\,i\boldsymbol{\sigma}\cdot\hat{k}_1], \tag{11}$$

$$\mathcal{N}_{2\gamma} = Z\,\frac{\alpha^2 g_{\pi\gamma\gamma}}{m_\pi}. \tag{12}$$

The amplitude $G(\mathbf{q},\mathbf{Q})$ originates with the current part of the electron-four-vector current, and $H(\mathbf{q},\mathbf{Q})$ with the spin part of the same current.

Taking into account multiple scattering of both electron and meson the expressions for the amplitudes become

$$G(\mathbf{q},\mathbf{Q}) = \int d^3r_e \int d^3r_\pi\, e^{i\mathbf{q}\cdot(\mathbf{r}_e-\mathbf{r}_\pi)}e^{-i\mathbf{Q}\cdot\mathbf{r}_\pi}\exp\left[i\chi_C(b_e) - \frac{1}{2}\sigma_\pi' T(\mathbf{b}_\pi, z_\pi)\right][\mathbf{E}_e(\mathbf{r}_e-\mathbf{r}_\pi)\times\mathbf{E}_A(\mathbf{r}_\pi)]\cdot\hat{k}_1, \tag{13}$$

$$H(\mathbf{q},\mathbf{Q}) = \int d^3r_e \int d^3r_\pi\, e^{i\mathbf{q}\cdot(\mathbf{r}_e-\mathbf{r}_\pi)}e^{-i\mathbf{Q}\cdot\mathbf{r}_\pi}\exp\left[i\chi_C(b_e) - \frac{1}{2}\sigma_\pi' T(\mathbf{b}_\pi, z_\pi)\right][\mathbf{E}_e(\mathbf{r}_e-\mathbf{r}_\pi)\cdot\mathbf{E}_A(\mathbf{r}_\pi)], \tag{14}$$

where $\mathbf{r}_e$ and $\mathbf{r}_\pi$ are the electron and pion coordinates. The nuclear $\mathbf{E}_A(\mathbf{r})$ and electron $\mathbf{E}_e(\mathbf{r})$ electric fields are the transverse parts of the corresponding fields. The distortion of the electron-wave function is described by the Coulomb-phase function $\chi_C(b_e)$, the distortion of the pion-wave function by the nuclear-thickness function $T(\mathbf{b}_\pi, z_\pi)$.

In the $G(\mathbf{q},\mathbf{Q})$ amplitude of Eq. (13) we recognize $\mathbf{E}_A(\mathbf{r}_\pi)$ as the radiated nucleus-electric field, and $\mathbf{E}_e(\mathbf{r}_e-\mathbf{r}_\pi)\times\hat{k}_1$ as the radiated electron-magnetic field, all in accordance with Eq. (4). The $H(\mathbf{q},\mathbf{Q})$ amplitude of Eq. (14) is associated with the spin current, and its parity is therefore opposite to that of the $G(\mathbf{q},\mathbf{Q})$ amplitude. Hence, it is built on the scalar product of the two electric fields.

Next, we give the definitions of the various functions entering the integrands of Eqs. (13) and (14). The transverse-electric field of the electron is

$$\mathbf{E}_e(\mathbf{r}) = \frac{1}{4\pi i}\frac{\gamma \mathbf{b}}{[\mathbf{b}^2+\gamma^2 z^2]^{3/2}}. \tag{15}$$

The γ dependence in this expression, which is in coordinate space, is compatible with the γ dependence in momentum space, Eq. (7). I apologize for the unconventional multiplicative constant. The transverse-electric field of the nucleus is in general associated with an extended-charge distribution $\hat{\rho}_{\rm ch}(r)$, which we normalize to unity,

$$\mathbf{E}_A(\mathbf{r}) = \frac{-Q(r)}{4\pi i}\frac{\mathbf{b}}{[\mathbf{b}^2+z^2]^{3/2}}, \tag{16}$$

$$Q(r) = 4\pi\int_0^r dr' r'^2 \hat{\rho}_{\rm ch}(r'), \tag{17}$$

and $Q(\infty)=1$. For a uniform-charge distribution with radius R_u,

$$Q(r) = \begin{cases} 1, & r > R_u, \\ (r/R_u)^3, & r < R_u. \end{cases} \tag{18}$$

Note that the fields of Eqs. (15) and (16) are defined to have opposite signs.

The expression for the Coulomb-phase function $\chi_C(b)$ in Eqs. (13) and (14) has been given by Glauber [2,7]. We employ the integral representation

$$\chi_C(b) = -2\frac{Z\alpha}{v}\int d^3r' \hat{\rho}_{\rm ch}(r')\left[\ln\left(\frac{|\mathbf{b}-\mathbf{b}'|}{2a}\right)\right], \tag{19}$$

where a is a cutoff parameter common to all amplitudes. For a point-charge distribution

$$\chi_{\rm pc}(b) = -2\frac{Z\alpha}{v}\ln(b/2a). \tag{20}$$

Additional information on the Coulomb-phase function can be found in Ref. [7], in particular expressions pertinent to uniform-charge distributions.

The pion distortion in Eqs. (13) and (14) is controlled by the parameter $\sigma_\pi' = \sigma_\pi(1-i\alpha_\pi)$ with σ_π the pion-nucleon-total-cross section. The target-thickness function $T(\mathbf{b},z)$ is defined as the integral along the pion trajectory of the nuclear-hadronic-matter density $A\hat{\rho}_{hd}(r)$ as seen by the pion,

$$T(\mathbf{b},z) = A\int_z^\infty dz' \hat{\rho}_{hd}(\mathbf{b},z'), \tag{21}$$

for a pion produced at $(\mathbf{b},z)$. The density $\hat{\rho}_{hd}(\mathbf{r})$ is normalized to unity.

The amplitudes $G(\mathbf{q},\mathbf{Q})$ and $H(\mathbf{q},\mathbf{Q})$ can be written on a more convenient form by making use of the operator replacements, $\boldsymbol{b}_e \to -i\nabla_q$ and $\boldsymbol{b}_\pi \to +i\nabla_Q$, as described in Ref. [3]. This operation leads to the decomposition

$$G(\mathbf{q},\mathbf{Q}) = K(\mathbf{q},\mathbf{Q})\,(\hat{\mathbf{q}}_\perp\times\hat{\mathbf{Q}}_\perp)\cdot\hat{k}_1 + L(\mathbf{q},\mathbf{Q})\,\hat{\mathbf{q}}_\perp\cdot\hat{\mathbf{Q}}_\perp, \tag{22}$$

$$H(\mathbf{q},\mathbf{Q}) = K(\mathbf{q},\mathbf{Q})\,\hat{\mathbf{q}}_\perp\cdot\hat{\mathbf{Q}}_\perp - L(\mathbf{q},\mathbf{Q})\,(\hat{\mathbf{q}}_\perp\times\hat{\mathbf{Q}}_\perp)\cdot\hat{k}_1, \tag{23}$$

with $\hat{\mathbf{q}}_\perp = \mathbf{q}_\perp/|\mathbf{q}_\perp|$ and $\hat{\mathbf{Q}}_\perp = \mathbf{Q}_\perp/|\mathbf{Q}_\perp|$.

The definitions of the scalar amplitudes $K(\mathbf{q},\mathbf{Q})$ and $L(\mathbf{q},\mathbf{Q})$ are, with $q_\parallel/\gamma \approx m_e$,

$$K(\mathbf{q},\mathbf{Q}) = \frac{m_e Q_\parallel}{(2\pi)^2}\int_0^\infty b_e db_e\, K_1(m_e b_e)\int_0^\infty b_\pi db_\pi\, I(b_\pi, Q_\parallel)2\pi \times\int_0^{2\pi} d\phi\, J_0(\sqrt{X})\{\cos\phi\}\exp[i\chi_C(B_e)], \tag{24}$$

$$L(\mathbf{q},\mathbf{Q}) = \frac{m_e Q_\parallel}{(2\pi)^2}\int_0^\infty b_e db_e\, K_1(m_e b_e)\int_0^\infty b_\pi db_\pi\, I(b_\pi, Q_\parallel)2\pi \times\int_0^{2\pi} d\phi\, J_0(\sqrt{X})\{-\sin\phi\}\exp[i\chi_C(B_e)], \tag{25}$$

with X and B_e as

$$X = (q_\perp b_e)^2 + (Q_\perp b_\pi)^2 - 2q_\perp b_e Q_\perp b_\pi\cos\phi, \tag{26}$$

$$B_e^2 = b_e^2 + b_\pi^2 + 2b_e b_\pi\cos(\phi+\phi_q-\phi_Q). \tag{27}$$

For general charge and matter distributions $I(b_\pi, Q_\parallel)$ is defined by the integral

$$I(b_\pi, Q_\parallel) = \frac{-2\pi i}{Q_\parallel}\int_{-\infty}^\infty dz[\hat{\mathbf{b}}_\pi\cdot\mathbf{E}_A(\mathbf{b}_\pi,z)] \times\exp\left[-izQ_\parallel - \frac{1}{2}\sigma_\pi' T(b_\pi,z)\right]. \tag{28}$$

For a point-charge distribution and neglect of meson rescattering it simplifies to

$$I_{\rm pc}(b_\pi, Q_\parallel) = K_1(Q_\parallel b_\pi), \tag{29}$$

where for negative values of the argument $K_1(-x) = -K_1(x)$.

In the Born approximation, i.e., for a nucleus point-charge distribution and with neglect of electron and pion distortions, the amplitudes $K(\mathbf{q},\mathbf{Q})$ and $L(\mathbf{q},\mathbf{Q})$ reduce to

$$K_B(\mathbf{q},\mathbf{Q}) = \frac{q_\perp}{\mathbf{q}_\perp^2+m_e^2}\cdot\frac{Q_\perp}{\mathbf{Q}_\perp^2+Q_\parallel^2}, \tag{30}$$

$$L_B(\mathbf{q},\mathbf{Q}) = 0, \tag{31}$$

with $-Q_\parallel = m_\pi^2/2K_\parallel$. In this case the integrals factorize. In fact, the functional dependence on the angles ϕ_q and ϕ_Q factorizes except in the Coulomb-phase-shift function.

IV. HADRONIC PRODUCTION

The hadronic contribution represents hadronic interactions between the high-energy photon and the nucleons in the nucleus. Those interactions can be described as exchange interactions where the exchanged particle, as in Fig. 2, is a ρ or an ω meson. For ω exchange, proton and neutron contributions add whereas for ρ exchange they subtract. In addition, the ρ interaction is weaker and we shall therefore neglect it altogether. The structure of the ω-exchange contribution is the same as that of photon exchange, except for the replacement of the Coulomb potential by the Yukawa potential. Hence, the

nuclear-electric field $\mathbf{E}_A(\mathbf{r})$ is replaced by the nuclear-ω field

$$\mathbf{E}_\omega(\mathbf{r}) = \nabla_b \frac{1}{4\pi i} \int d^3r' \hat{\rho}_{hd}(\mathbf{r}') \frac{e^{-m_\omega|\mathbf{r}-\mathbf{r}'|}}{|\mathbf{r}-\mathbf{r}'|}, \tag{32}$$

where $A\hat{\rho}_{hd}(\mathbf{r})$ is the hadronic-density distribution as seen by the ω meson. The ω propagator can be displayed by rewriting this expression as

$$\mathbf{E}_\omega(\mathbf{r}) = \frac{1}{i(2\pi)^3} \nabla_b \int d^3q e^{-i\mathbf{q}\cdot\mathbf{r}} \frac{1}{\mathbf{q}^2 + m_\omega^2} S_0(\mathbf{q}) \tag{33}$$

with $S_0(\mathbf{q})$ the nuclear form factor,

$$S_0(\mathbf{q}) = \int d^3r e^{i\mathbf{q}\cdot\mathbf{r}} \hat{\rho}_{hd}(\mathbf{r}). \tag{34}$$

Unfortunately, high-energy photoproduction of pseudoscalar mesons by nucleons is not well described by the meson exchanges. But Guidal *et al.* [8] have shown that by Reggeizing those exchanges a good description of data can be obtained. Reggeization means replacing the ω-pole factor

$$\mathcal{P}_\omega = \frac{1}{t - m_\omega^2} \tag{35}$$

with its Reggeized version, which is

$$\mathcal{P}_\omega(s,t) = \left(\frac{s}{s_0}\right)^{\alpha_\omega(t)-1} \frac{\pi\alpha'_\omega}{\sin(\pi\alpha_\omega(t))} \frac{1}{\Gamma(\alpha_\omega(t))} \frac{-1 + e^{-i\pi\alpha_\omega(t)}}{2}. \tag{36}$$

The parametrization of the ω trajectory, $\alpha_\omega(t)$, has been determined through comparison with photoproduction data [8].

For an ambitious calculation that aims at including the full Regge structure the definition of the nuclear-ω field becomes

$$\begin{aligned}\mathbf{E}_\omega(\mathbf{r}) &= \frac{1}{i(2\pi)^3} \nabla_b \int d^3q e^{-i\mathbf{q}\cdot\mathbf{r}} \frac{1}{m_\omega^2} S_0(\mathbf{q}) \hat{\mathcal{P}}_\omega(\mathbf{q}^2) \\ &= \frac{i}{2\pi^2 m_\omega^2} \mathbf{b} \int dq\, q^4 S_0(q) \hat{\mathcal{P}}_\omega(q^2) \left[\frac{j_1(qr)}{qr}\right],\end{aligned} \tag{37}$$

with

$$\hat{\mathcal{P}}_\omega(\mathbf{q}^2) = \mathcal{P}_\omega(\mathbf{q}^2)/\mathcal{P}_\omega(\mathbf{q}^2 = 0), \tag{38}$$

and $S_0(\mathbf{q})$ the nuclear form factor of Eq. (34). There could also be other form factors beside the Regge factor. The $\mathbf{q}^2$ dependence of the Regge factor is much weaker than that of the nuclear factor. Neglecting it altogether leads to a simple expression for the nuclear-ω field,

$$\mathbf{E}_\omega(\mathbf{r}) = \frac{1}{im_\omega^2} \nabla_b \hat{\rho}_{hd}(\mathbf{r}). \tag{39}$$

The ω-exchange amplitude is decomposed as follows:

$$\mathcal{M}_\omega = -i\mathcal{N}_\omega [G_\omega(\mathbf{q},\mathbf{Q}) - H_\omega(\mathbf{q},\mathbf{Q})\, i\boldsymbol{\sigma}\cdot\hat{k}_1], \tag{40}$$

$$\mathcal{N}_\omega = A \frac{\alpha g_{\omega\pi\gamma} g_{\omega NN}}{4\pi m_\pi} m_\omega^2 \mathcal{P}_\omega(0). \tag{41}$$

Pure ω exchange corresponds to $m_\omega^2 \mathcal{P}_\omega(0) = -1$. The functions of Eq. (40) are defined in complete analogy with the two-photon exchange amplitudes,

$$\begin{aligned}G_\omega(\mathbf{q},\mathbf{Q}) = \int d^3r_e \int d^3r_\pi\, e^{i\mathbf{q}\cdot(\mathbf{r}_e - \mathbf{r}_\pi)} e^{-i\mathbf{Q}\cdot\mathbf{r}_\pi} \exp\Big[i\chi_C(b_e) \\ - \frac{1}{2}\sigma'_\pi T(\mathbf{b}_\pi, z_\pi)\Big] [\mathbf{E}_e(\mathbf{r}_e - \mathbf{r}_\pi) \times \mathbf{E}_\omega(\mathbf{r}_\pi)]\cdot\hat{k}_1,\end{aligned} \tag{42}$$

$$\begin{aligned}H_\omega(\mathbf{q},\mathbf{Q}) = \int d^3r_e \int d^3r_\pi\, e^{i\mathbf{q}\cdot(\mathbf{r}_e - \mathbf{r}_\pi)} e^{-i\mathbf{Q}\cdot\mathbf{r}_\pi} \exp\Big[i\chi_C(b_e) \\ - \frac{1}{2}\sigma'_\pi T(\mathbf{b}_\pi, z_\pi)\Big] [\mathbf{E}_e(\mathbf{r}_e - \mathbf{r}_\pi)\cdot\mathbf{E}_\omega(\mathbf{r}_\pi)].\end{aligned} \tag{43}$$

The definitions of $G_\omega(\mathbf{q},\mathbf{Q})$ and $H_\omega(\mathbf{q},\mathbf{Q})$ in Eqs. (42) and (43) parallel the definitions of $G(\mathbf{q},\mathbf{Q})$ and $H(\mathbf{q},\mathbf{Q})$ in Eqs. (13) and (14). To get from the latter to the former we replace $\mathbf{E}_A(\mathbf{r}_\pi)$ with $\mathbf{E}_\omega(\mathbf{r}_\pi)$. In exactly the same way we define $K_\omega(\mathbf{q},\mathbf{Q})$ and $L_\omega(\mathbf{q},\mathbf{Q})$ to get the decomposition

$$G_\omega(\mathbf{q},\mathbf{Q}) = K_\omega(\mathbf{q},\mathbf{Q})\, (\hat{\mathbf{q}}_\perp \times \hat{\mathbf{Q}}_\perp)\cdot\hat{k}_1 + L_\omega(\mathbf{q},\mathbf{Q})\, \hat{\mathbf{q}}_\perp\cdot\hat{\mathbf{Q}}_\perp, \tag{44}$$

$$H_\omega(\mathbf{q},\mathbf{Q}) = K_\omega(\mathbf{q},\mathbf{Q})\, \hat{\mathbf{q}}_\perp\cdot\hat{\mathbf{Q}}_\perp - L_\omega(\mathbf{q},\mathbf{Q})\, (\hat{\mathbf{q}}_\perp \times \hat{\mathbf{Q}}_\perp)\cdot\hat{k}_1. \tag{45}$$

However, the replacement of $\mathbf{E}_A(\mathbf{r}_\pi)$ by $\mathbf{E}_\omega(\mathbf{r}_\pi)$ makes the structure functions connected with ω exchange quite different from those connected with photon exchange. In general, $L_\omega(\mathbf{q},\mathbf{Q})$ is small and may be neglected.

V. FACTORIZATION

The formulas given so far apply to arbitrary nuclei and arbitrary momentum transfers $\mathbf{Q}_\perp$ and $\mathbf{q}_\perp$, as long as they remain much smaller than the longitudinal momenta k_1 and K. The tricky point in their evaluation is that the integrations over $\mathbf{r}_e$ and $\mathbf{r}_\pi$ are intertwined, as the electron interacts with both nucleus and meson. However, in some circumstances the integrations factorize.

Consider production of η *mesons* at 11 GeV, and start with the Coulomb terms $K(\mathbf{q},\mathbf{Q})$ and $L(\mathbf{q},\mathbf{Q})$ of Eqs. (24) and (25). The cutoff in the b_e integration is set by the inverse of the electron mass $1/m_e \approx 390$ fm, and the cutoff in the b_η integration by the inverse of the longitudinal momentum transfer $2K_\parallel/m_\eta^2 \approx 14$ fm. The only coupling between the b_e and b_η dependencies is in the argument, Eq. (27), of the Coulomb-phase function. In view of the small overlap region, we may here neglect the dependence on b_η. As a result, the integrands of Eqs. (24) and (25) factorize, and the function $L(\mathbf{q},\mathbf{Q})$ vanishes after integration over the ϕ variable. These arguments are weakened when we consider momentum transfers $\mathbf{q}_\perp$ so large that there are strong oscillations in the b_e integrand. Then the main contributions to the Coulomb integral come from regions much closer to the nucleus.

In the factorized approximation

$$L(\mathbf{q},\mathbf{Q}) = 0, \tag{46}$$

$$K(\mathbf{q},\mathbf{Q}) = F_C(\mathbf{q}) F_A(\mathbf{Q}), \tag{47}$$

with the functions $F_C(\mathbf{q})$ and $F_A(\mathbf{Q})$ defined by

$$F_C(\mathbf{q}) = \int d^3r_e\, e^{i[\mathbf{q}\cdot\mathbf{r}_e+\chi_C(b_e)]}\, \hat{\mathbf{q}}_\perp \cdot \mathbf{E}_e(\mathbf{r}_e), \tag{48}$$

$$F_A(\mathbf{Q}) = \int d^3r_\eta\, e^{-i\mathbf{Q}\cdot\mathbf{r}_\eta} \hat{\mathbf{Q}}_\perp \cdot \mathbf{E}_A(\mathbf{r}_\eta) \exp\left[-\frac{1}{2}\sigma'_\eta T(\mathbf{b}_\eta, z_\eta)\right]. \tag{49}$$

The function $F_C(\mathbf{q})$ describes Coulomb scattering by the electron, and for a nuclear-point-charge distribution it can be integrated exactly, Refs. [3,9]. The $F_A(\mathbf{Q})$ is the Coulomb contribution (one-photon exchange) to η-nucleus photoproduction.

In the hadronic contribution the integration over b_η is limited to the nuclear region. Thus, in this case the integrals always factorize, so that $L_\omega(\mathbf{q}, \mathbf{Q}) = 0$ and

$$K_\omega(\mathbf{q}, \mathbf{Q}) = F_C(\mathbf{q}) F_\omega(\mathbf{Q}), \tag{50}$$

$$F_\omega(\mathbf{Q}) = \int d^3r_\eta\, e^{-i\mathbf{Q}\cdot\mathbf{r}_\eta} \hat{\mathbf{Q}}_\perp \cdot \mathbf{E}_\omega(\mathbf{r}_\eta) \exp\left[-\frac{1}{2}\sigma'_\eta T(\mathbf{b}_\eta, z_\eta)\right]. \tag{51}$$

The sum of Coulomb and hadronic contributions can be written as

$$G(\mathbf{q}, \mathbf{Q}) + G_\omega(\mathbf{q}, \mathbf{Q}) = \sum_\lambda [\hat{\mathbf{q}}_\perp \cdot \mathbf{e}_\lambda\, F_C(\mathbf{q})]\{(\hat{\mathbf{Q}}_\perp \times \hat{k}_1) \cdot \mathbf{e}_\lambda [F_A(\mathbf{Q}) + F_\omega(\mathbf{Q})]\}, \tag{52}$$

where the sum runs over the two photon-polarization vectors orthogonal to $\hat{k}_1$, or $\hat{q}$. For the sum $H(\mathbf{q}, \mathbf{Q}) + H_\omega(\mathbf{q}, \mathbf{Q})$ the expression is the same but with $\hat{\mathbf{q}}_\perp \cdot \mathbf{e}_\lambda$ replaced by $(\hat{\mathbf{q}}_\perp \times \hat{k}_1) \cdot \mathbf{e}_\lambda$.

The two terms in the last bracket of Eq. (52) represent the η-nucleus photoproduction amplitude initiated by photons of polarization $\mathbf{e}_\lambda$. The first term $F_A(\mathbf{Q})$ is the Coulomb-photoproduction amplitude, the second term $F_\omega(\mathbf{Q})$ the hadronic-photoproduction amplitude. It is also important to note that the photons radiated by the electron are transverse photons, not Coulomb photons.

In pion-electroproduction the hadronic amplitudes factorize, but the Coulomb amplitudes do not. Hence, the pion-electroproduction amplitude will not have a decomposition as in Eq. (52).

VI. SHADOWING

The hadronic contribution is modified by shadowing, a multiple scattering contribution where the initial photon is first converted into a ρ meson, which in a subsequent collision with another nucleon creates the pion. This phenomenon is described in detail in Ref. [10].

In the hadronic term the high-energy photon produces the final-state pion through ω-meson exchange with a single nucleon. The corresponding amplitude is proportional to $f_\omega(\gamma N \to \pi N)$. In the shadowing term the high-energy photon first creates a ρ meson by diffractive production on a nucleon. This step is proportional to $f_P(\gamma N \to \rho N)$. In the second step the ρ meson collides with another nucleon creating a π meson through ω-meson exchange. This step is proportional to the amplitude $f_\omega(\rho N \to \pi N)$. Now, if the hadronic interactions of photons proceed via the ρ meson, we expect the relation

$$f_P(\gamma N \to \rho N) f_\omega(\rho N \to \pi N) = f_P(\rho N \to \rho N) f_\omega(\gamma N \to \pi N), \tag{53}$$

where $f_P(\rho N \to \rho N)$ is the diffractive ρ-nucleon-scattering amplitude. We remark that the ρ meson is off its mass shell in two of the amplitudes, one on each side. It is assumed that the off-shell factors cancel out.

The amplitude relation (53) leads to a replacement of the ω field, Eq. (39), by

$$\mathbf{E}_\omega(\mathbf{r}) = \frac{1}{i m_\omega^2} \nabla_b \hat{\rho}_{hd}(\mathbf{r}) \left\{1 - \frac{1}{2}\sigma'_\rho \int_{-\infty}^{z} dz' n(\mathbf{b}, z') e^{i\Delta_\rho(z'-z)} \times \exp\left[-\frac{1}{2}\sigma'_\rho \int_{z'}^{z} dz'' n(\mathbf{b}, z'')\right]\right\}, \tag{54}$$

with $n(\mathbf{r}) = A\hat{\rho}_{hd}(\mathbf{r})$. The second term inside the brackets is the shadowing term. The intermediate ρ meson is produced at z' and the final-state pion at z. Between these two points, the distortion of the wave is due to ρ-meson scattering. The longitudinal momentum transfer in the $\gamma N \to \rho N$ reaction at z' is $\Delta_\rho = m_\rho^2/2K_\parallel$. The longitudinal momentum transfer in the $\rho N \to \pi N$ reaction at z is $\Delta_\pi = (m_\pi^2 - m_\rho^2)/2K_\parallel = -\Delta_\rho - Q_\parallel$. In the direct hadronic term the longitudinal momentum transfer to the pion is $-Q_\parallel = m_\pi^2/2K_\parallel$. This phase factor is outside the ω field $\mathbf{E}_\omega(\mathbf{r})$. So is the pion distortion, Eqs. (44) and (45).

VII. NUCLEAR ω-EXCHANGE AMPLITUDE

Our previous article [3] presented analytic and numerical details of the pure-Coulomb amplitudes. What remains to complete the picture is a numerical study of the ω-exchange amplitude.

The structure of the nuclear-density distribution tells us that the ω field $\mathbf{E}_\omega(\mathbf{r})$ of Eq. (39) is concentrated at the rim of the nucleus. In fact, for a uniform-nuclear-density distribution of radius R_u

$$\mathbf{E}_\omega(\mathbf{r}) = \frac{i}{m_\omega^2} \frac{3}{4\pi R_u^3} \frac{\mathbf{b}}{r} \delta(r - R_u). \tag{55}$$

This expression corresponds to inserting a uniform-density-form factor

$$S_u(q) = \frac{3 j_1(q R_u)}{q R_u} \tag{56}$$

into Eq. (37), ignoring the Regge factor. With a uniform-density distribution alone, the integral of Eq. (37) is not properly convergent. However, a nuclear density with realistic surface-density distribution does give a properly convergent integral. Adding the Regge-form factor further improves the convergence.

The investigation of the structure of the ω field conveniently starts with the associated function $V(r)$, obtained after angular

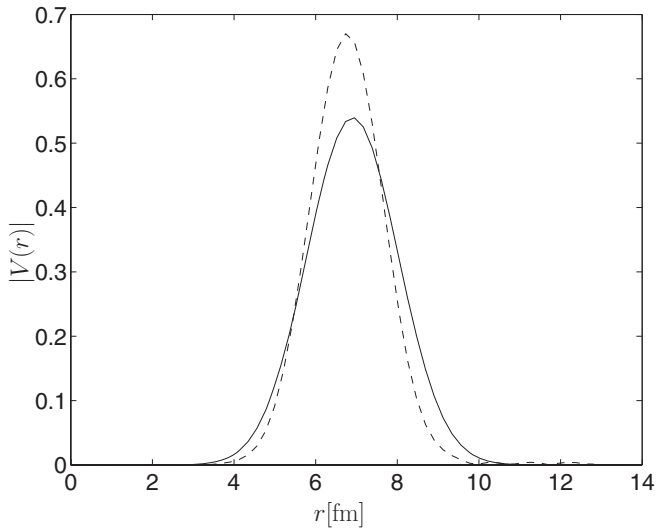

FIG. 3. Graph describing the radial distribution of $|V(r)|$ of Eq. (57) for lead nuclei, in units of inverse fm; dashed curve corresponds to nucleus-form factor, solid curve to nucleus- plus Regge-form factors.

integration of Eq. (37),

$$V(r) = \frac{1}{\pi}\int_0^\infty dq(qr)^3 S(q) j_1(qr), \tag{57}$$

where r is the radial parameter and where the form factor $S(q)$ may or may not contain the Regge factor. The relation to the ω field is

$$\mathbf{E}_\omega(\mathbf{r}) = \frac{i}{2\pi m_\omega^2}\frac{\mathbf{b}}{r^4} V(r). \tag{58}$$

In Fig. 3 the absolute value of $V(r)$ is graphed for two cases: nucleus-form factor alone and nucleus- plus Regge-form factors, the latter as in Eq. (37). We see that the values of $V(r)$ are restricted to the surface region of the nucleus, $r \approx R_u = 6.5$ fm, as for the uniform-nucleus-density distribution, Eq. (55). The distribution involving the nucleus-form factor alone (dashed line) is slightly higher and narrower than the one with the added Regge-form factor (solid line). Moreover, the integral of $V(r)$ over the radial parameter r is the same in both cases,

$$\int_0^\infty dr\, V(r) = \frac{3}{2}S(0) = \frac{3}{2}, \tag{59}$$

and indeed, the same as for the uniform-density distribution. We refer to the Appendix for a proof of this identity.

Next, we turn to the ω-exchange amplitude of Eq. (51). It can be rewritten as

$$F_\omega(\mathbf{Q}) = \frac{Q_\perp}{m_\omega^2}\int_0^\infty dr\, W(\mathbf{Q}, r) V(r), \tag{60}$$

with $V(r)$ defined as in Eq. (57) and with

$$W(\mathbf{Q}, r) = \int_{-1}^{1} du(1-u^2)\frac{J_1(Q_\perp r\sqrt{1-u^2})}{Q_\perp r\sqrt{1-u^2}} \times \exp\left[-iQ_\parallel ru - \frac{1}{2}\sigma' T(r\sqrt{1-u^2}, ru)\right]. \tag{61}$$

Furthermore, the target thickness function $T(b, z)$ is the integral of the hadronic density along the pion trajectory, Eq. (21), and the meson-production point in the nucleus is at $(\mathbf{b}, z)$.

In order to illustrate the meaning of the above expressions, consider a simplified case. Ignoring meson distortion, integration of Eq. (61) gives

$$W(\mathbf{Q}, r) = \frac{2j_1(Qr)}{Qr}, \tag{62}$$

and choosing, in addition, a uniform-density distribution

$$V_u(r) = \tfrac{3}{2}\delta(r - R_u) \tag{63}$$

results in a nuclear ω-exchange amplitude

$$F_\omega(\mathbf{Q}) = \frac{Q_\perp}{m_\omega^2}\frac{3j_1(Qr)}{Qr} = \frac{Q_\perp}{m_\omega^2}S_u(Qr), \tag{64}$$

an expression that should, by now, be familiar.

The ω-exchange amplitude of Eq. (60) is obtained by averaging the function $W(\mathbf{Q}, r)$ over a function $V(r)$ which is concentrated at the surface region, where $W(\mathbf{Q}, r)$ itself is rapidly varying. This is demonstrated by the solid curve in Fig. 4(a), where $W(\mathbf{Q}, r)$ is plotted for *η-meson* production at momentum transfer $Q_\perp = 2Q_\parallel$. The dashed curve represents the no-distortion case of Eq. (62). As is obvious, distortion severely cuts down the contribution from the interior of the nucleus leading to a strong variation in the surface region, i.e., in the neighborhood of $r = 6.5$ fm.

In Fig. 4(b) the amplitude $m_\omega^2|F_\omega(\mathbf{Q})|/Q_\perp$ is graphed as a function of $Q_\perp$, with $Q_\perp$ measured in units of the fixed-longitudinal-momentum transfer $Q_\parallel$. The solid curve is the result of the full calculation and the dotted curve, almost indistinguishable from the solid one, represents a calculation where the Regge amplitude is evaluated in the forward direction. We conclude that in applications to heavy nuclei, this approximation of the Regge amplitude is excellent, as anticipated in Ref. [3]. The dashed curve refers to vanishing distortion and consequently represents the form factor of the nucleus. The position of the minimum around $9Q_\parallel$ is related to the zero in the form factor.

In the application to pion production the longitudinal-momentum transfer to the pion, $Q_\parallel(m_\pi)$, is much smaller than the one for η production, $Q_\parallel(m_\eta)$. Therefore, the structure of $|W(\mathbf{Q}, r)|$ in Fig. 4(a) becomes independent of $Q_\perp$ and $Q_\parallel$, and the no-absorption curve is a straight line. The curves of Fig. 4(b) are also virtually straight lines with minima far outside the figure.

In the application to η' production, on the other hand, the longitudinal-momentum transfer to the η' meson, $Q_\parallel(m_{\eta'})$, is much larger than the one for η production, $Q_\parallel(m_\eta)$. The effect is to produce a minimum in $|W(\mathbf{Q}, r)|$ around $r \approx 10$ fm and a suppression of the maximum. The momentum distribution of Fig. 4(b) has a first minimum already at $r \approx 3Q_\parallel$ and three more up to $r \approx 10Q_\parallel$.

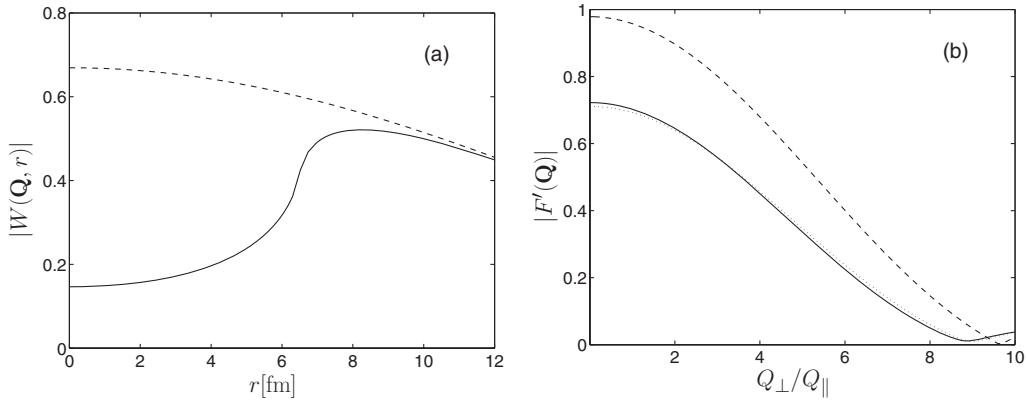

FIG. 4. Graphs describing (a) the radial distribution of $|W(\mathbf{Q}, r)|$ of Eq. (61) for $Q_\perp = 2Q_\parallel$, and (b) the $Q_\perp$ momentum-transfer distribution of the ω-exchange amplitude $m_\omega^2|F_\omega(\mathbf{Q})|/Q_\perp$ of Eq. (60). Dashed curves refer to vanishing absorption, Eqs. (62) and (64). This is all for η-meson production on lead.

VIII. CROSS-SECTION DISTRIBUTIONS

The unpolarized-cross-section distribution as derived in Ref. [3] reads

$$\frac{d\sigma}{d^2k_{2\perp}d^2K_\perp dk_{2\parallel}} = \frac{1}{\pi K_\parallel}\left(\frac{Z\alpha^2 g_{\pi\gamma\gamma}}{m_\pi}\right)^2 [|K(\mathbf{q},\mathbf{Q}) + \mathcal{R}K_\omega(\mathbf{q},\mathbf{Q})|^2 + |L(\mathbf{q},\mathbf{Q}) + \mathcal{R}L_\omega(\mathbf{q},\mathbf{Q})|^2], \tag{65}$$

with the coupling constant $g_{\pi\gamma\gamma}$ determined by the radiative decay width of the pion

$$\Gamma(\pi^0 \to \gamma\gamma) = \tfrac{1}{4}\pi\alpha^2 g_{\pi\gamma\gamma}^2 m_\pi, \tag{66}$$

and with $\mathcal{R}$ the ratio of the coupling constants of Eqs. (12) and (41),

$$\mathcal{R} = -\mathcal{N}_\omega/\mathcal{N}_{2\gamma}. \tag{67}$$

The parameter $\mathcal{R}$ depends only weakly on atomic number so we do not gain relative strength for the Coulomb term by going to heavier nuclei. The advantage is instead that the cross-section values themselves grow as Z^2. An interesting feature of Eq. (65) is that in the unpolarized cross-section distributions K and L amplitudes do not interfere. The sign of $\mathcal{R}$ must be determined by experiment.

The transverse momenta in Eq. (65) are restricted to the regions $q_\perp, Q_\perp \ll k_1, k_2, K$. For cross-section distributions such that $Q_\perp R_u \approx 1$, nuclear structure becomes important and numerical evaluation necessary. We have also stressed that depending on the value of $q_\perp/m_e$, integrals may or may not factorize. The complicated functional dependencies make a general overview difficult. For this reason we concentrate on production of pions and η mesons in the Coulomb region, which is of special importance to the PrimEx experiment.

π-meson production. Pion electroproduction at 11 GeV/c was investigated in Ref. [3], with emphasis on the double-Coulomb region, where $Q_\perp \approx |Q_\parallel| = 0.85$ MeV/c and $q_\perp \approx m_e = 0.52$ MeV/c. In this particular case there is, in the Coulomb amplitude, a strong overlap between the impact-parameter domains of pion and electron. As a consequence the electroproduction amplitude does not factorize and the predictions differ considerably from the Born approximation. Non-factorization means that the pion-nucleus-*photo*production cross section is not a factor of the pion-nucleus-*electro*production cross section.

However, non-factorization does not mean we cannot determine the pion-decay constant $g_{\pi\gamma\gamma}$. We can, as long as we have a reliable theory for the cross-section distribution and as long as the hadronic contribution is much smaller than the Coulomb contribution.

In Ref. [3] the relative size of Coulomb and hadronic amplitudes was estimated. Here, we first assume pure ω exchange and neglect electron and pion distortions. Then, at the double peak, the ratio of Coulomb to hadronic amplitude strengths becomes

$$R_\pi = \left[\frac{Z\alpha^2 g_{\pi\gamma\gamma}}{m_\pi}\frac{1}{2Q_\parallel^2}\right]\Big/\left[\frac{A\alpha g_{\omega\pi\gamma}g_{\omega NN}}{4\pi m_\pi}\frac{1}{m_\omega^2}\right] = 110. \tag{68}$$

The numerical value refers to lead nuclei. Taking Regge exchange instead of ω exchange implies dividing by $|\mathcal{P}_\omega(0)m_\omega^2| = 0.102$, which is the strength of Regge relative to pure ω exchange. The new ratio $R_\pi = 1080$ is so large that it should be easy to isolate the Coulomb contribution from the hadronic background, making a determination of $g_{\pi\gamma\gamma}$ realistic.

Photoproduction of pseudoscalar mesons by protons, including the Coulomb term, was investigated in Ref. [11], and photoproduction by nuclei most recently in Refs. [12,13].

η-meson production. Production of η mesons is at 11 GeV/c simpler to calculate than production of π mesons. The double-Coulomb region is now the region where $Q_\perp \approx |Q_\parallel| = 14$ MeV/c, and $q_\perp \approx m_e = 0.52$ MeV/c. Consequently, overlap between the integration domains of the η- and electron-impact-parameter variables is small. The factorization discussed in Sec. V applies and the cross-section distribution contains the factor

$$|F_C(\mathbf{q})|^2|F_A(\mathbf{Q}) + F_\omega(\mathbf{Q})|^2. \tag{69}$$

The first factor in Eq. (69) is the squared Coulomb amplitude of the electron. Its analytic form is given in Refs. [3,9]. It is not the usual Coulomb-scattering amplitude since it describes exchange of transverse photons, not Coulomb photons. In the Coulomb factor $F_C(\mathbf{q})$ the longitudinal momentum $q_\parallel$ enters in the combination $q_\parallel/\gamma \approx m_e$. This factor exhibits a Primakoff-peak structure in the variable $q_\perp$ with a peak value at $q_\perp \approx m_e$.

The second factor in Eq. (69) is the squared η-nucleus-photoproduction amplitude. This amplitude has two parts: the Coulomb amplitude $F_A(\mathbf{Q})$ and the hadronic amplitude $F_\omega(\mathbf{Q})$. Assuming ω exchange and neglecting electron and pion rescattering the ratio R_η of Coulomb to hadronic amplitudes is algebraically the same as the ratio for pions, Eq. (68), but with all π indices replaced by η indices. For lead nuclei $R_\eta = 1.8$ with ω exchange and $R_\eta = 18$ with Regge exchange. The Coulomb amplitude dominates but only weakly. For an accurate determination of $g_{\eta\gamma\gamma}$ higher energies are needed.

η'-meson production. At 11 GeV/c the double-Coulomb region in η' production is the region where $Q_\perp \approx |Q_\parallel| = 43$ MeV/c, and $q_\perp \approx m_e = 0.52$ MeV/c. As for η-meson production the factorization discussed in Sec. V applies as well as Eq. (69). The second factor in Eq. (69) is now the squared η'-nucleus-photoproduction amplitude. Assuming ω exchange and neglecting electron and pion rescattering the ratio $R_{\eta'}$ of Coulomb to hadronic amplitudes is algebraically the same as the ratio for pions, Eq. (68), but with all π indices replaced by η' indices. For lead nuclei $R_{\eta'} = 0.30$ with ω exchange and $R_{\eta'} = 2.9$ with Regge exchange. Consequently, a determination of $g_{\eta'\gamma\gamma}$ is not possible at this energy.

ACKNOWLEDGMENT

I would like to thank J. M. Laget for a useful correspondence.

APPENDIX

In the Hankel integral formula Eq. (59) the crucial integral is

$$\frac{1}{\pi}\int_0^\infty dr(qr)^3 j_1(qr) = q^3(-\partial_q)\frac{1}{q}\frac{1}{2\pi}\int_{-\infty}^{\infty} drr\sin(qr) = q^3\partial_q\frac{1}{q}\,\partial_q\delta(q) = -q\delta'(q) + q^2\delta''(q) = 3\delta(q). \tag{A1}$$

The last step is valid only when the operators are averaged over functions which are finite at $q = 0$. The q integration of Eq. (59) starts at $q = 0$. In order to avoid an endpoint singularity we must, before evaluating the integral, rewrite it as an integral from minus infinity to plus infinity. The above integral identity can be extended to Bessel functions of arbitrary order, as

$$\frac{1}{2\pi}\int_{-\infty}^{\infty} dr(qr)^{n+2} j_n(qr) = q^{2n+2}\left[-q\frac{\partial}{\partial q}\right]^{n+1}\delta(q) \tag{A2}$$

$$= (-1)^{n+1}(2n+1)!!\,\delta(q). \tag{A3}$$

We end with an alternative method for deriving Eqs. (22) and (23). Decompose the unit vector $\hat{b}_e$ along the unit vector $\hat{q}$, which here stands for the impact-plane component $\boldsymbol{q}_\perp$ of $\boldsymbol{q}$, i.e., $\hat{q} = \boldsymbol{q}_\perp/|\boldsymbol{q}_\perp|$,

$$\hat{b}_e = [\hat{b}_e\cdot\hat{q}]\,\hat{q} + [\hat{b}_e\cdot(\hat{k}\times\hat{q})]\,\hat{k}\times\hat{q} = \cos(\varphi_e)\,\hat{q} + \sin(\varphi_e)\,\hat{k}\times\hat{q}. \tag{A4}$$

We perform the same decomposition for $\hat{b}_\pi$ but along $\hat{Q}$ and with angle φ_π. This gives

$$\hat{b}_e\cdot\hat{b}_\pi = \cos\varphi\,\hat{q}\cdot\hat{Q} + \sin\varphi\,(\hat{q}\times\hat{Q})\cdot\hat{k}, \tag{A5}$$

$$(\hat{b}_e\times\hat{b}_\pi)\cdot\hat{k} = -\sin\varphi\,\hat{q}\cdot\hat{Q} + \cos\varphi\,(\hat{q}\times\hat{Q})\cdot\hat{k}, \tag{A6}$$

with $\varphi = \varphi_e - \varphi_\pi$.

[1] E. Hadjimichael and S. Fallieros, Phys. Rev. C **39**, 1438 (1989).
[2] R. J. Glauber, in *Lectures in Theoretical Physics*, edited by W. E. Brittin and L. G. Dunham, Vol. 1 (Interscience, New York, 1959), p. 315; in *High-Energy Physics and Nuclear Structure*, edited by S. Devons (Plenum, New York, 1970), p. 207.
[3] G. Fäldt, Phys. Rev. C **83**, 044606 (2011).
[4] A. Gasparian *et al*., Proposal E-02-103, 2001.
[5] G. Fäldt, Nucl. Phys. B **43**, 591 (1972).
[6] L. Landau and E. Lifchitz, *Théorie des champs* (Éditions Mir, Moscou, 1970).
[7] G. Fäldt, Phys. Rev. D **2**, 846 (1970).
[8] M. Guidal, J.-M. Laget, and M. Vanderhaegen, Nucl. Phys. A **627**, 645 (1997).
[9] G. Fäldt and U. Tengblad, Phys. Rev. C **79**, 014607 (2009); G. Fäldt, *ibid.* **82**, 037603 (2010).
[10] D. R. Yennie, in *Hadronic Interactions of Electrons and Photons*, edited by J. Cumming and H. Osborn (Academic Press, New York, 1971), p. 321.
[11] J.-M. Laget, Phys. Rev. C **72**, 022202(R) (2005).
[12] S. Gevorkyan, A. Gasparian, L. Gan, I. Larin, and M. Khandaker, Phys. Rev. C **80**, 055201 (2009).
[13] M. M. Kaskulov and U. Mosel, Phys. Rev. C **84**, 065206 (2011).